PHILOSOPHICAL TRANSACTIONS OF THE ROYAL SOCIETY A MATHEMATICAL, PHYSICAL & ENGINEERING SCIENCES

Laue Diffraction as a Tool in Dynamic Studies: Hydrolysis of a Transiently Stable Intermediate in Catalysis by Trypsin

Paul T. Singer, Robert P. Carty, Lonny E. Berman, Ilme Schlichting, Ann Stock, Arne Smalas, Zhouping Cai, Walter F. Mangel, Keith W. Jones and Robert M. Sweet

Phil. Trans. R. Soc. Lond. A 1992 **340**, 285-300
doi: 10.1098/rsta.1992.0067

Laue diffraction as a tool in dynamic studies: hydrolysis of a transiently stable intermediate in catalysis by trypsin

By Paul T. Singer[1], Robert P. Carty[2], Lonny E. Berman[3], Ilme Schlichting[4], Ann Stock[5], Arne Smalås[6], Zhouping Cai[1], Walter F. Mangel[1], Keith W. Jones[7] and Robert M. Sweet[1]

[1] *Biology Department,* [7] *Department of Applied Science and* [3] *National Synchrotron Light Source, Brookhaven National Laboratory, Upton, New York 11973, U.S.A.*

[2] *Department of Biochemistry, State University of New York Health Science Center at Brooklyn, Brooklyn, New York 11203, U.S.A.*

[4] *Rosenstiel Basic Medical Science Center, Brandeis University, Waltham, Massachusetts 02254, U.S.A.*

[5] *Center for Advanced Biotechnology and Medicine, Piscataway, New Jersey 08854-5638, U.S.A.*

[6] *Institute of Mathematics and Physical Sciences, University of Tromsö, N-9000 Tromsö, Norway*

A transiently stable intermediate in trypsin catalysis, guanidinobenzoyl-Ser-195 trypsin, can be trapped and then released by control of the pH in crystals of the enzyme. This effect has been investigated by static and dynamic white-beam Laue crystallography. Comparison of structures determined before and immediately after a pH jump reveals the nature of concerted changes that accompany activation of the enzyme. Careful analysis of the results of several structure determinations gives information about the reliability of Laue results in general. A study of multiple exposures taken under differing conditions of beam intensity, crystal quality, and temperature revealed information about ways to control damage of specimens by the X-ray beam.

1. Introduction

A motive for three-dimensional structure analysis of enzymes is to understand their catalytic mechanism. Enzymes appear to work in a very mechanical way. One can propose that to know the structure of this machine in detail will help one to understand how each structural component contributes to catalysis. This idea can be expanded in several ways. In static crystallographic studies, natural or artificial components of the catalytic pathway can be introduced to the enzyme. Crystal structures of complexes of an enzyme with substrates, inhibitors or pseudo-substrates provide accessible routes to substantial knowledge about the mechanism of the enzyme.

However, this approach has a limitation: it is difficult to learn something about interesting small molecule substrates or effectors one might add to the enzyme because such molecules are likely to undergo a transformation catalysed by the

Phil. Trans. R. Soc. Lond. A (1992) **340**, 285–300
Printed in Great Britain

enzyme. The species one would like to see will disappear more quickly than data can be measured to determine the structure. A compromise is to use substrate molecules that have been modified in a way that will still allow them to be recognized by the enzyme, but prevents the reaction from proceeding beyond a certain point. Another possibility for static studies is to omit some component of a reaction mixture to prevent the reaction from occurring.

Ideally, one would like to view the catalytic mechanism in action; time-resolved crystallography has the potential to do just that. One could hope to trigger a reaction in a crystal of an enzyme, the course of which could then be followed by repetitive measurement of diffraction data, perhaps sufficient to define the complete structure. Single crystal diffraction with the use of a polychromatic X-ray beam is a possible tool for such rapid measurement of these data.

This method, known as Laue-diffraction crystallography, is described in some detail by other authors in this volume (see also reviews by Moffat (1989) and Hajdu & Johnson (1990)). It can be summarized: the method depends upon the white beam of X-rays that is available from a synchrotron radiation source; because all of the flux of X-rays can be used for a single exposure, very short exposure times are possible; the wide range of wavelengths ensures that a significant portion of reciprocal space is sampled concurrently, so that few exposures are required; and methods and computer programs have been developed to produce high-quality data for crystal structure analysis. The theoretical time-resolution limit depends ultimately on the brightness of the synchrotron. We will demonstrate time resolution in the 10 ms to 1 s régime in work done at the NSLS, Brookhaven. Workers at the Cornell University Synchrotron have demonstrated usable data taken in 120 ps (Szebenyi, 1988). Thus, Laue diffraction may be a good choice for dynamic problems that push the limits of other more conventional data-collection methods.

Unfortunately, the time-resolution of the dynamic result actually depends on relations among parameters other than the sampling time for the diffraction measurements. These are the speed of the trigger and the rate of the reaction to be observed. The resulting structures will always be blurred by the convolution of these effects; additional phenomena will confuse the result further. The detail in the structure will depend upon the quality and completeness of the diffraction measurements. Spatial and temporal inhomogeneities will be introduced into the crystal by non-ideal characteristics of the triggering mechanism. For example, if the trigger is a flash of ultraviolet or visible light, then absorption of the light by the specimen will result in an intensity gradient across the crystal. If the trigger requires diffusion of a substrate into the crystal, the moving front will necessarily produce a concentration gradient with its concomitant inhomogeneity in triggering. The crux of the problem is synchronization of the reaction. One would like all diffracting molecules to remain in exactly the same conformation throughout the experiment. We have described the difficulty of getting all the molecules in a crystal even to initiate a reaction simultaneously. Things only get worse: reactions proceed in a statistical manner with the synchrony diverging with time.

A serious requirement, and thus a potential limitation, is the absolute demand for high-quality crystals. It is no coincidence that the science of topography uses polychromatic, still-crystal X-ray photographs to locate strain and structure in macroscopic crystals. The reverse of this is that a white-beam photograph reveals every imperfection in the crystal specimen. Any crack in a crystal produces multiple or misshapen spots. High mosaic spread in the crystal, from whatever cause, will

PHILOSOPHICAL TRANSACTIONS OF THE ROYAL SOCIETY A MATHEMATICAL, PHYSICAL & ENGINEERING SCIENCES

yield streaky spots. Furthermore, any of these imperfections is readily produced by radiation damage or the stress of mounting in a flow cell or of being subjected to sudden changes in buffer or temperature. During pioneering experiments in dynamic crystallography, Hajdu *et al.* (1987) (see also Stoddard *et al.* 1991; Reynolds *et al.* 1988; H. D. Bartunik, personal communication) observed an order–disorder–order phenomenon in crystals of glycogen phosphorylase *b*. The course of the reaction to be studied actually disrupted the crystal so badly that the data could not be measured accurately enough for a structure determination. This sort of disorder leads, at best, to uninterpretable regions in the density map, and at worst to useless diffraction images.

It will pay to explore methods that allow dynamic structural study of reaction mechanisms. Topics that should be considered are the sort of diffraction experiment to perform, the perfection of crystals required for the diffraction experiment, crystal damage that might occur during X-ray exposure, exposure times that are possible, the quality of structure that can be obtained, and for triggered reactions, the effect of the trigger on the course of the reaction and on the structural results that follow. These explorations are some of the burden of this report.

We have embarked on a dynamic study of catalysis by the enzyme trypsin. Our initial goal was to probe the steps that comprise deacylation of a transiently stable intermediate during catalysis: GB(guanidinobenzoyl)-trypsin (Mangel *et al.* 1990, space group $P2_12_12_1$; $a = 63.74$ Å†, $b = 63.54$ Å and $c = 68.93$ Å) (GB-trypsin is trypsin esterified at Ser 195 with GB). The key to the experiment was: first, that the acyl intermediate was stable for a very long time at pH 5.5; secondly, the rate of deacylation is higher at high pH with a $t_{\frac{1}{2}}$ of approximately 1 h at pH 8.9. Crystals of the acylated enzyme were mounted in a flow cell so that the pH of the surrounding medium could be changed quickly and easily. In this mounting we used the white X-ray beam produced by the NSLS to measure diffraction data from a low-pH acylated crystal, from the same crystal immediately after the pH had been raised to 8.9, and then again after 90 min incubation at the higher pH.

To examine some of the questions suggested above – perfection of crystals, crystal damage, exposure times, the quality of structures, and the effect of the pH jump that was to serve as a trigger – we also determined several structures of a static form of benzamidine-inhibited native trypsin by both Laue and monochromatic techniques. To serve as a static control for future dynamic experiments, non-acylated trypsin was used. Crystals of trypsin grown at pH 5.5 were analysed by monochromatic synchrotron radiation. A second set of crystals was grown at pH 5.5, incubated for 24 h at pH 9.0, and returned to pH 5.5, after which monochromatic diffraction data were measured. This experiment was designed to test the effect of the pH change on these crystals. Next, a crystal of trypsin at pH 5.5 was used for Laue-data collection. Finally, the same crystal was subjected to a rapid pH-jump to 9.0 and data were collected again. The purpose of the latter experiments was to establish the feasibility of combining the pH-jump technique with the white-beam Laue method for trypsin, and to measure structural changes that occur in the native enzyme. This would serve as a control for the experiment with the acyl-enzyme.

† 1 Å = 10^{-10} m = 10^{-1} nm.

PHILOSOPHICAL TRANSACTIONS OF THE ROYAL SOCIETY A MATHEMATICAL, PHYSICAL & ENGINEERING SCIENCES

2. Laue-diffraction measurements

Beamlines X25 and X26-C at Brookhaven Laboratory's NSLS were used for the white-beam diffraction measurements. Beamline X25 (Berman *et al.* 1992), powered by a 27-pole wiggler magnet, was developed by a consortium of scientists interested in high-flux scattering measurements. Beamline X26-C has been developed by the Department of Applied Science at Brookhaven Laboratory and has been used in the past for gas-phase atomic physics experiments and fluorescence measurements of trace elements in biological specimens. Each has a similar emission spectrum from the NSLS X-ray ring, and each beam is focused by a toroidal mirror. The range of usable wavelengths is approximately 0.7 Å to 1.7 Å, limited at the low end by the critical energy cutoff of the mirrors and at the high end by Be windows and graphite attenuators in the beamline.

Summary of Laue experiments

Two completely different experiments were performed with Laue data, as mentioned in §1. Structures of two different states of benzamidine-inhibited native trypsin were determined from a single crystal with data collected at the wiggler beamline, X25. Data were collected from a single crystal at low pH. This structure will be named Lo-pH Laue. The buffer surrounding this crystal was replaced with buffer at a higher pH and data were collected again; this structure will be named Hi-pH Laue. Also, structures were determined at several time-points before and after raising the pH of a single crystal of GB-trypsin with data from beamline X26-C. The low-pH structure will be referred to as t_0; the structure determined 3 min after the pH was raised is t_3, and the structure determined 90 min after that is t_{90}. Details are described below.

Crystal preparation and flow-cell construction

All crystals were grown as GB-trypsin as described before (Mangel *et al.* 1990). For the native trypsin studies, the stabilization buffer was 3 M ammonium sulphate, 0.05 M benzamidine (a non-covalent inhibitor often used in trypsin studies to prevent autolysis), 0.1 M sodium citrate, pH 5.5. The ammonium ion in the buffer quantitatively and rapidly drives deacylation of GB-trypsin to yield native trypsin crystals. The high-pH buffer was 3 M ammonium sulphate, 0.05 M benzamidine, 0.1 M Tris.HCl, pH 8.9. For crystals of GB-trypsin the low pH stabilization buffer was 2.5 M $MgSO_4$, 0.1 M sodium acetate, pH 5.5; the high pH stabilization buffer was 2.5 M $MgSO_4$, 0.1 M Tris.HCl, pH 8.9.

All crystals were equilibrated against the low-pH stabilization buffers as described above and then were transferred to 0.7 mm quartz capillaries. The crystals were allowed to settle against a plug of cotton fibres and, after crude alignment, were secured in place by a second plug. Fine-bore polyethylene tubing was inserted into each end to provide flow of buffer and sealed with wax or epoxy cement. The capillaries were themselves fastened to a semicircular brass yoke, which could be mounted on a goniometer head. Buffer flow (20 $cm^3\ h^{-1}$) was driven by gravity. In each case the pH jump was accomplished by transfer of the supply tubing from low to high pH buffer. A bubble was introduced into the tubing so the precise moment of the buffer change could be observed in the televised microscope.

Table 1. *Data reduction statistics for Laue data reduction*

structure	beamline	number of packs	mean intra-pack R factor (%)	total observations	unique reflections	percent of total to 1.8 Å	R factor for all data (%)	R factor within 0.1 Å
Lo-pH	X25	6	3.3	38500	14700	58	16.0	12.9
Hi-pH	X25	6	4.1	35600	15600	62	18.1	14.0
t_0	X26-C	5	4.6	24500	13100	52	18.9	12.8
t_3	X26-C	7	3.9	41000	18600	74	14.8	11.0
t_{90}	X26-C	7	4.8	36700	16800	67	15.1	10.9

Data collection

Crystals were mounted with one crystal axis oblique to the camera rotation axis by 20–25°. Between five and seven exposures were collected for each data set, spanning 90° of reciprocal space. Three or four exposures were made on each portion of the specimen crystal and then the crystal was translated along the camera axis to place a fresh portion of the crystal in the X-ray beam. This strategy provided several-fold redundancy in the data, allowing a reasonable fraction of the complete reciprocal lattice to be sampled without the need for accurate adjustment of spindle or arc settings (Clifton *et al.* 1991). The cotton fibres surrounding the crystal made such alignment extremely difficult.

The camera was an Enraf-Nonius Arndt/Wonacott rotation camera modified for control by a microcomputer and for mounting on a Klinger X95 optical rail. A 0.15 mm collimator was used. The rotary film carousel held up to eight standard 5 in × 5 in cassettes allowing rapid film-changing. Specimen-to-film distance was 75 mm. Rapid shuttering was accomplished by use of a 3 in diameter disc of alternate layers of 2 mm thick copper, lead and copper. The disc was mounted directly onto the shaft of a stepping motor; radial slits in the disc could be rotated through the beam to provide single pulses of X-rays as short as 2 ms. The duration of the pulses at various motor speeds was calibrated by use of a storage oscilloscope and an ionization chamber placed downstream of the shutter.

The two different beamlines required markedly different exposure times: typically 25 ms at a synchrotron ring current of 130 mA (beamline X25) and 800 ms at 180 mA (beamline X26-C). In both cases a 1.5 mm graphite filter was placed in the beam to remove longer wavelength photons; preliminary work had indicated that this practice greatly increased the lifetime of the crystals in the beam.

Individual film packs generally consisted of five sheets of Kodak DEF film, labelled A–E. Films were digitized using an Optronics P-1000 rotating-drum scanner with 50 μm beam size and density range 0–2.

Data reduction

All film packs were processed with the Daresbury suite of programs (Helliwell *et al.* 1989). Data reduction statistics are given in table 1. Briefly, the program GENLAUE is used to fit the various camera constants and crystal setting angles to the observed spot locations. Residuals were typically in the range of 25–50 μm. Several film packs were overexposed and required special treatment. For these packs first the C film was used for refinement of all parameters, including the unit cell. The process was then repeated for the entire film pack, using values from pack C for the crystal missetting angles ϕ_x and ϕ_y. This results in substantially lower residuals

PHILOSOPHICAL TRANSACTIONS OF THE ROYAL SOCIETY A MATHEMATICAL, PHYSICAL & ENGINEERING SCIENCES

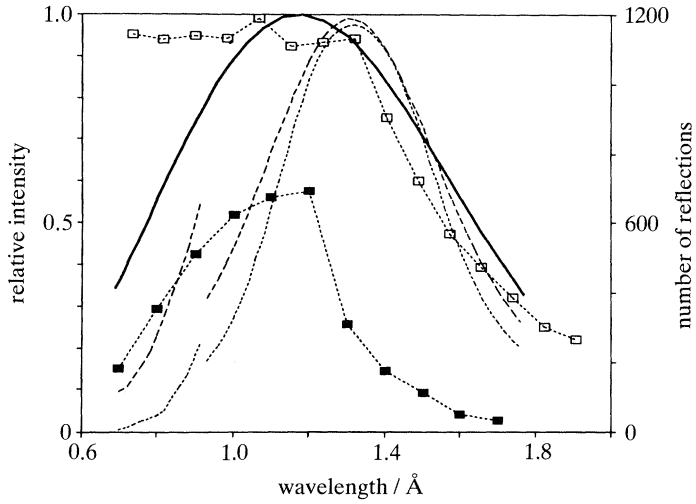

Figure 1. Normalization curves for X25 (– – –) and X26-C (···); measured spectrum of X25 (——); measured reflections (■); predicted reflections (□).

because the C, D, and E films in the pack have much lower background than the A and B films.

The intra-filmpack scaling, as performed by the program AFSCALE, resulted in merging R factors between 2.5 and 5%. ($R = \Sigma|I_0 - \langle I\rangle|/\Sigma\langle I\rangle$, where $\langle I\rangle$ is the mean of averaged observations I_0.) There was high correlation between larger numbers of measurements in a film pack and lower merging R factors. The film-to-film merging R factors were lower for the C–D and D–E film pairs (data not shown), consistent with the observation that these films carried the better data. The choice of the C film for the initial run of GENLAUE was a compromise between film quality and the number and distribution of reflections found on the film.

The program LAUENORM was used to perform the wavelength normalization and to scale together data from several film packs. Since a typical experiment consisted of three separate time points, all these data were used to calculate the wavelength normalization curve with the NORMALISE option. Subsequently, the SCALE option was used to apply the normalization curve to the film packs for each individual time point. While the merging R factor for intra-filmpack scaling was *ca.* 5%, the interpack R factor following wavelength normalization was larger: *ca.* 15% (table 1). Note that the R factor for only those measurements taken at essentially the same wavelength (last column) are considerably lower, indicating that the wavelength normalization process is a significant source of error. In figure 1 are shown, for beamline X25 and for the Lo-pH Laue structure, the relations among the normalization curve determined by LAUENORM, the measured spectrum of the beam produced by X25, the number of reflections measured, and the number of reflections that could have been measured at each wavelength.

In this figure the curve that represents the number of predicted reflections includes harmonic multiples, which comprise 10% of the total. This curve and that representing the number of observed reflections parallel one another at long wavelengths. The deficit between the two arises from the generally poor signal-to-noise ratio for Laue films. However, one also can see that a huge fraction of the data that might have been observed at short wavelengths simply have not been. This

might be explained by the physics of the experiment, as follows. The strength of scattering increases strongly with increasing wavelength. Absorption by the film/detector also increases strongly with increasing wavelength. And finally, the spectrum of the source is weaker in the short-wavelength régime than in the long. Long-wavelength radiation contributes substantially to X-ray background because it is scattered efficiently and absorbed well by the film, but to relatively few, widely spaced reflections. Short-wavelengths contribute to reflections that correspond to poor scattering and poor detection.

We were also concerned that some portion of the missing data might come from regions of reciprocal space that were missed by our multiple exposure protocol. This possibility was examined by producing a three-dimensional scatter plot of the reflections in reciprocal space, to be viewed in stereo. While the missing data at low resolution were clearly visible, there were no additional large regions of empty space.

3. Monochromatic data measurement

Monochromatic diffraction data were measured from crystals of trypsin with the FAST area diffractometer installed at beamline X12-C at the NSLS at Brookhaven National Laboratory (Sweet *et al.* 1990). Parameters of the data collection can be enumerated: the wavelength used was 1.1 Å; the collimator aperture was 0.2 mm; specimen-to-detector distance was 75 mm; detector inclination $\theta = 25°$; rotation increments were 0.1°; exposure times were 8–10 s; specimens were kept at approximately 18 °C; and the detector was run at gain settings SETD 71. Incident beam intensities were monitored with an ionization chamber mounted to follow the collimator. These monitor counts were used during data reduction with the computer program MADNES (Messerschmidt & Pflugrath 1987) to correct each image for variations in the beam intensity. Each reflection was fitted by a learned profile by the method of Kabsch (1988).

As described previously in §1, monochromatic data were measured from crystals that had been treated two different ways. One crystal was maintained in a stabilization buffer at pH 5.5; this experiment will be called Lo-pH Mono. The X-ray beam used for data collection was smaller than the crystal, so three different sections of the single crystal were used for the complete data collection. The other crystals were transferred from pH 5.5 to 9.0 for 24 h, after which they were returned to low pH for data collection; this structure will be referred to as Hi-pH Mono. A total of three different sections of two different crystals were used for data collection. In each case, several sweeps of data were taken at different oblique settings to provide a complete survey of reciprocal space. These sweeps were divided into sectors containing roughly 1000 reflections each for scaling. The program FS (Weissman 1982), which fits a Fourier surface to the area of the detector as a scale factor for each sector, was used for scaling of the data. Statistics for data reduction are given in table 2. Unit cell parameters were refined by the program MADNES during data reduction and were essentially identical to those found previously (Mangel *et al.* 1990).

4. Model refinement against Laue and monochromatic data

The starting point for the refinement of all seven structures was the 2 Å model of GB-trypsin described previously (Mangel *et al.* 1990), except that the GB group was removed from Ser 195 for the four benzamidine-inhibited structures. These were

PHILOSOPHICAL TRANSACTIONS OF THE ROYAL SOCIETY A MATHEMATICAL, PHYSICAL & ENGINEERING SCIENCES

Table 2. *Data reduction statistics for synchrotron high-resolution monochromatic data reduction measured to* 1.5 Å *resolution*

sample	total measured	unique reflections	percent of total	R
Low-pH Mono	125400	36900	83	0.089
Hi-pH Mono	110900	33900	76	0.077

Table 3. *Refinement statistics from X-PLOR for three structures: at pH* 5.5, (t_0); 3 min *after the jump to pH* 8.9 (t_3); *and* 90 min *after the pH jump* (t_{90})

	t_0		t_3		t_{90}	
reflections[a]...	10600		15000		13600	
method[b]...	CG	SA	CG	SA	CG	SA
initial R	0.269	0.222	0.254	0.192	0.257	0.193
final R	0.222	0.204	0.192	0.178	0.193	0.179
mean B factor						
all	15.6	15.1	18.3	18.9	18.6	19.4
protein	12.4	12.1	14.5	15.0	15.0	15.6
solvent	37.3	34.8	43.8	45.0	42.9	44.1
GB group	4.4	6.6	7.5	8.9	13.0	12.0
RMS deviation from ideal						
bonds/Å	0.017	0.015	0.014	0.012	0.015	0.013
angles/deg	3.5	3.2	3.0	2.7	3.1	2.8
GB occupancy	—	0.88	—	0.74	—	0.73

[a] All refinements were done with data where $F > 5\sigma$ over the resolution range 5.0–1.8 Å. In all cases, the model contained 1890 non-hydrogen atoms, of which 248 were solvent.

[b] CG, conjugate gradient; SA, simulated annealing. See text for details.

refined using the TNT program suite (Tronrud & Ten Eyck 1987); final weights were adjusted to yield reasonable statistics for the root mean square (RMS) deviations from geometric ideality. Care was taken during each phase of the refinement to relax geometric constraints sufficiently to fit the diffraction data as well as possible, and then to reimpose them to give a chemically reasonable structure. We believe this approach minimizes bias imparted by the starting model.

The models for the dynamic Laue experiment were refined further using the program X-PLOR 2.1 (Brünger 1990). The initial refinement was performed using the Powell (conjugate gradient) minimizer, first for atomic coordinates, and then for individual isotropic B factors. Subsequently, the simulated annealing (SA) protocol was used to refine the model further, with an initial temperature of 3000 K and 50 steps of 0.5 fs for each 25 K decrease. Finally, several more cycles of atomic coordinate and B factor energy minimization were performed. The refinement statistics are summarized in table 3.

The SA refinement moved water molecules around significantly, very often replacing one water molecule with another. In addition, the process often removed a solvent molecule from one site and replaced it at a site where none had existed in the original model. We exploited this by placing any new water molecules from each of the three new models into the starting model and repeating the entire refinement

Table 4. *Statistics at the end of refinement of high and low pH Laue and monochromatic structures*
(There were 1630 protein atoms in each refinement.)

structure	total number of atoms	resolution range/Å	number of reflections	R_F	bond length error/Å	bond angle error/deg
Lo-pH Mono	1812	5–1.5	36900	19.5	0.020	2.7
Hi-pH Mono	1759	5–1.5	33900	20.8	0.018	2.7
Lo-pH Laue	1813	5–1.8	14700	17.7	0.018	2.9
Hi-pH Laue	1759	5–1.8	15600	19.0	0.019	2.9

process. That these water assignments were reasonable was confirmed by inspection of electron-density maps, as well as by examination of the refined B factors and occupancies.

5. Comparison of Laue and monochromatic results

Monochromatic and polychromatic diffraction studies were performed to test conditions of the dynamics experiment. Two monochromatic structure analyses were performed. In one case, crystals of the benzamidine-inhibited enzyme were transferred directly to pH 5.5 stabilization buffer prior to mounting (Lo-pH Mono). In the second case, crystals of benzamidine-inhibited trypsin were cycled through the pH rise and fall that is used to trigger the GB hydrolysis from GB-trypsin (Hi-pH Mono).

Two Laue-data structures were determined from a single crystal of benzamidine-inhibited trypsin. The first was at the low pH of crystal growth, pH 5.5 (Lo-pH Laue); the second was at pH 8.9, with the data having been measured approximately three minutes after the pH had been raised in a flow cell (Hi-pH Laue). Although a detailed comparison of these structures with the similar monochromatic structures is underway, a number of features can be reported in the context of these proceedings. The structures fit the data well at this stage in refinement. Some refinement statistics are displayed in table 4. Since benzamidine was in the buffer, it was found in the active site in each structure. There are apparent differences in the details of the Laue versus monochromatic structures, especially in the disposition of fixed water molecules and some polar side chains on the surface of the protein molecules. The principal difference was that fewer fixed solvent molecules could be defined for the Laue-data structures. This was at least in part a result of there being many fewer data for these structure determinations.

Representative views from these structures are shown in figure 2. These maps were calculated with the benzamidine molecules omitted from the structure-factor calculation. The density for benzamidine is visible in both the monochromatic and the Laue electron-density maps. One also can see that the constellations of water molecules in the figures are very similar. This leads one to be optimistic about the prospects of identifying subtle features in maps determined by Laue methods.

Only a small number of structures have been refined from Laue data. These include glycogen phosphorylase (Hajdu *et al.* 1987), glucose isomerase (Farber *et al.* 1988), turkey lysozyme (Howell *et al.* 1990), tomato bushy-stunt virus (Campbell *et al.* 1990), chymotrypsin (Stoddard *et al.* 1991), and the P21/GTP complex (Schlichting

PHILOSOPHICAL TRANSACTIONS OF THE ROYAL SOCIETY A MATHEMATICAL, PHYSICAL & ENGINEERING SCIENCES

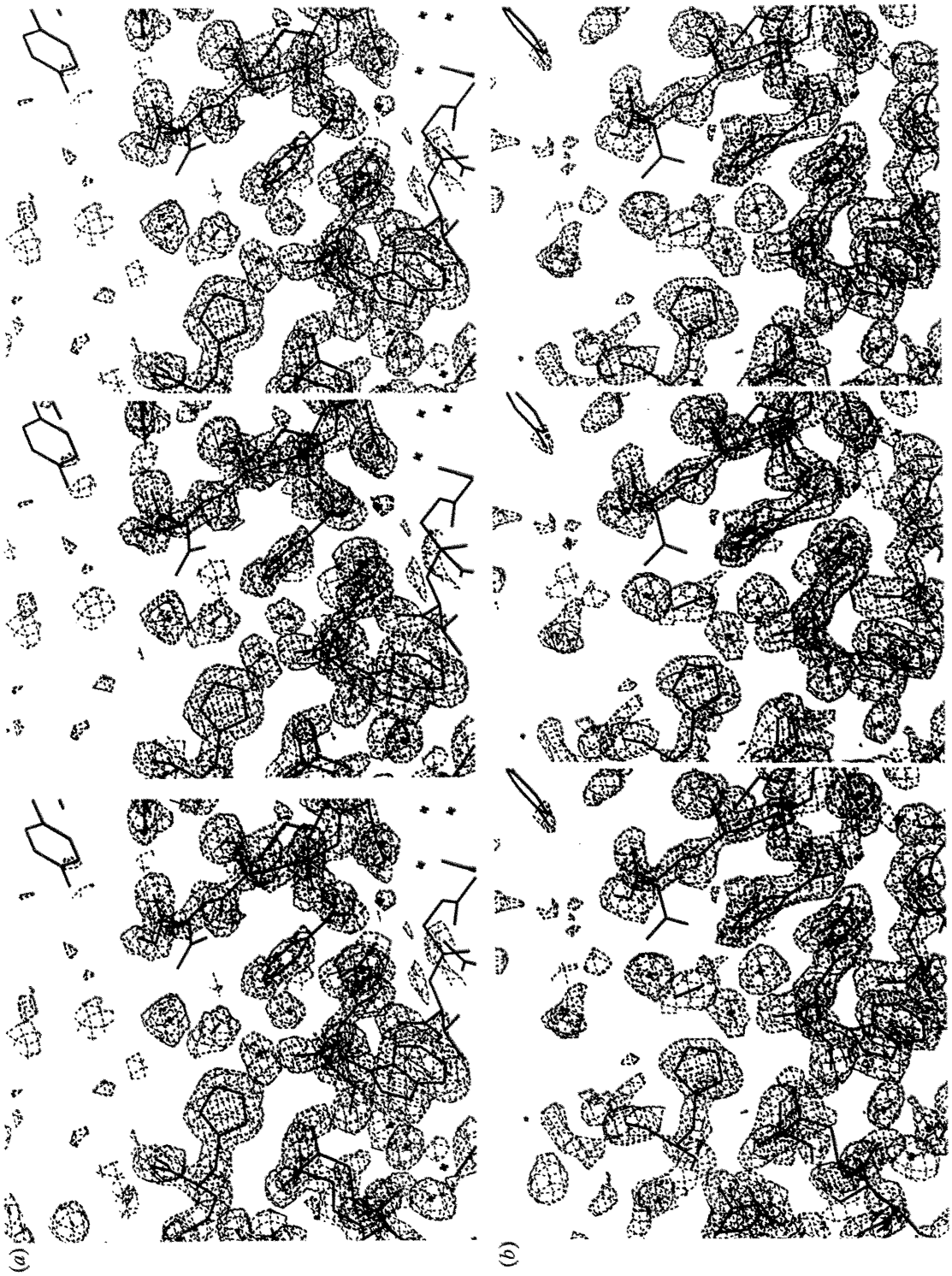

Figure 2. For caption see facing page.

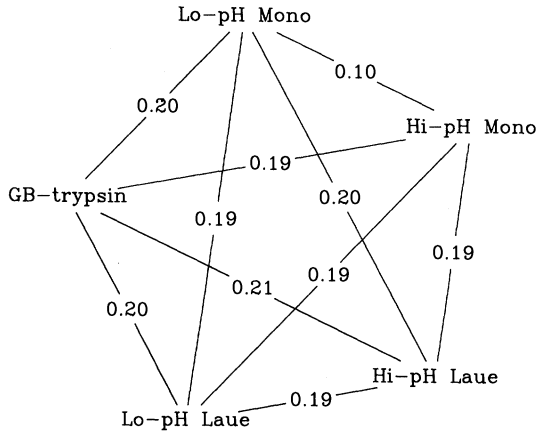

Figure 3. Mean distances in ångstroms among approximately 1600 protein-only atoms with occupancies greater than 0.5.

et al. 1990). None of these has been determined to better than 2.5 Å resolution. Therefore these trypsin structures, which include between one third and a half of the possible data between 2.0 and 1.8 Å resolution, not only are the highest resolution structures yet determined by the method, but also provide proof that the method can yield structures of this quality.

The most gratifying result, to the extent that these combined monochromatic and Laue structure determinations represent control experiments for the final dynamics experiments, was that there was little difference among them. The similarities can be displayed in a figure that shows mean shifts in atomic positions in comparisons among the four structures determined in this experiment and the original GB-trypsin structure determined at 2.0 Å resolution (figure 3). One can see that the two monochromatic benzamidine-trypsin structures agree to within 0.1 Å and that all other mean deviations are in the range of 0.2 Å.

6. Changes in GB-trypsin caused by a pH jump

As was described in §1, structures were determined for a crystal of GB-trypsin in a flow cell at pH 5.5 (the pH at which the crystals were grown and mounted), approximately 3 min after the pH was raised to 8.9, and then again 90 min later. Refinement of these structures and interpretation of the resulting models and electron-density maps is in progress and will be reported when the work is finished.

The effect one might expect to see in this case is likely to be small: The pH rise should be accompanied by the removal of a hydrogen atom from the $N_{\epsilon 2}$ atom of imidazole and a rearrangement of the hydrogen bonds to that atom. Figure 4 shows views of the enzyme's active site from each of the three time-points at the present stage of refinement; statistics for these refinements are shown in table 3. For GB-

Figure 2. Views in the trypsin active-site region. Densities are $2|F_o|-|F_c|$. Benzamidine was omitted from the phase calculation. (*a*) Hi-pH mono; (*b*) Hi-pH Laue. These figures and figure 4 are a stereo triptych for the left, right and left eyes, viewing from the left. The left-most pair can be viewed with a stereo-viewer; the right-most by crossing the eyes.

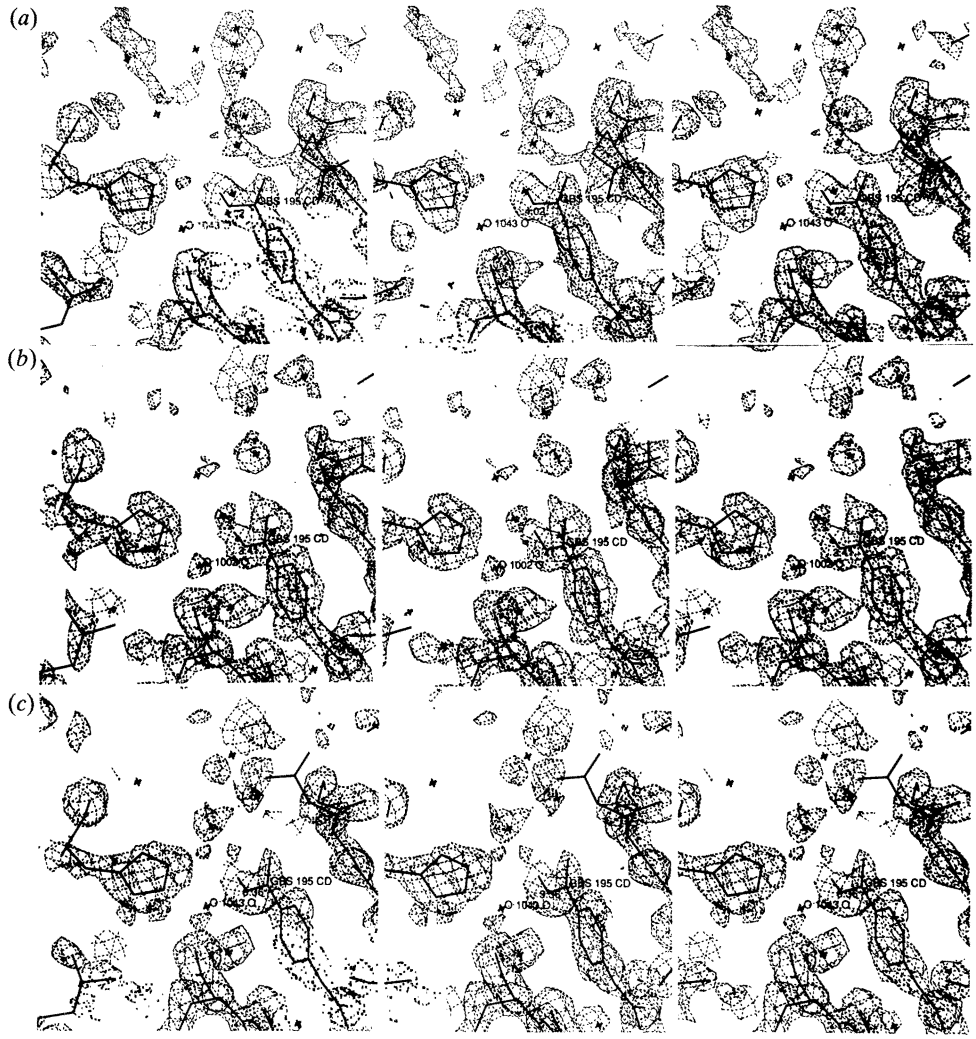

Figure 4. Trypsin active site region. Densities are $2|F_0|-|F_c|$. (*a*) t_0, (*b*) t_3, (*c*) t_{90}. To view stereoscopically the image must be magnified by 150%.

trypsin, the overall *B* factor rises approximately 25% upon raising of the pH, even before bond breakage. Our in-crystal kinetic studies led us to believe that the GB group would have been largely gone after 90 min. Possibly the GB occupancy figure at t_{90} does not distinguish properly between covalently and non-covalently bound guanidinobenzoate: note the *B* factor of the GB group. (See Stoddard *et al.* (1991) for another example of a similar problem.)

It is difficult to see whether there are significant shifts in the protein atoms around the active site, but there are clearly rearrangements of water molecules that might participate in the hydrolysis of the GB group. The refinement suggests that a weakly occupied water molecule moves gradually closer to the carbonyl carbon atom of the scissile ester bond as time progresses. The electron densities suggest that the occupancy for this water molecule is extremely low at t_0, but significantly high at the

higher pH. These differences in water structure at the two pHs will help one to rationalize the difference in stability of the ester bond. Further calculations will suggest the limits of confidence in the positions and occupancies of those molecules.

7. Damage of crystals by the X-ray beam

An irksome problem for protein crystallographers is the damage that their specimens suffer in an X-ray beam. The availability of synchrotron sources has partly relieved this problem: paradoxically, for most protein crystals, two to five times as many data can be collected from a single specimen as with conventional sources. Also, higher-resolution data can be obtained because radiation damage in protein crystals seems to involve a slow diffusion-controlled process. Data can be gathered on a synchrotron before these processes damage the crystalline order.

A possible extension of this idea is that because the polychromatic X-ray beam from a synchrotron source is extremely intense, Laue diffraction could, even better than methods that use monochromatic synchrotron radiation, be used to defeat the crystal-damage problem. This is an especially interesting question in the context of our wanting to monitor the time-course of reactions in a crystal by the taking of repetitive exposures. However, while using the very intense focused beam at NSLS beamline X25, we observed a surprisingly shorter life-time of some crystals. To test this phenomenon we have taken hundreds of photographs from dozens of crystals on the two NSLS beamlines described in §2. We have examined the photographs carefully and are able to make qualitative conclusions from the experiment; eventually we will be able to report quantitative results from the data we have taken.

Three questions were asked: Are there contrasting effects of two X-ray beams that differ in intensity by 1–2 orders of magnitude, the more intense of which has a power of on the order of 10^2 W mm^{-2}? What is the effect of cooling specimens from room temperature to near freezing? Does it pay to mount the crystal in contact with a volume of liquid that might aid in conduction of heat away from the specimen or in diffusion away of reactive products of the absorption of X-rays?

Three different specimen crystals were used: crystals of the orthorhombic trypsin described in this report, of tetragonal hen egg-white lysozyme, and of hexagonal glutathione synthase (Kato *et al.* 1989). The goal was to mimic a dynamic experiment and to measure successive identical photographs from the same volume of the specimen crystal so that the time-course of crystal damage could be observed in detail. Eight series were taken from each crystal: two different beamlines, two different temperatures and two different mounting protocols, wet (with a generous droplet of liquid in contact with the crystal) and dry (with as little liquid touching the crystal as was possible). Trypsin crystals were found to be so robust that results from them were not used in the final analysis. In general, we chose an exposure that would be suitable for intensity-data collection. An initial crude quantitation of damage is the number of frames of high quality data that can be measured.

In the joint contexts of our desire to follow the time-course of a reaction, and of the international drive for brighter and brighter X-ray sources, we believe that there is an interesting result. There is a systematic tendency for the less intense X-ray beam to allow one to take a larger number of images before crystal damage makes the images unusable for quantitative data. Crystals of glutathione synthase were seen to be exquisitely sensitive to X-radiation at room temperature. In the case of several crystals photographed on the wiggler beamline, crystals evidently

PHILOSOPHICAL TRANSACTIONS OF THE ROYAL SOCIETY A MATHEMATICAL, PHYSICAL & ENGINEERING SCIENCES

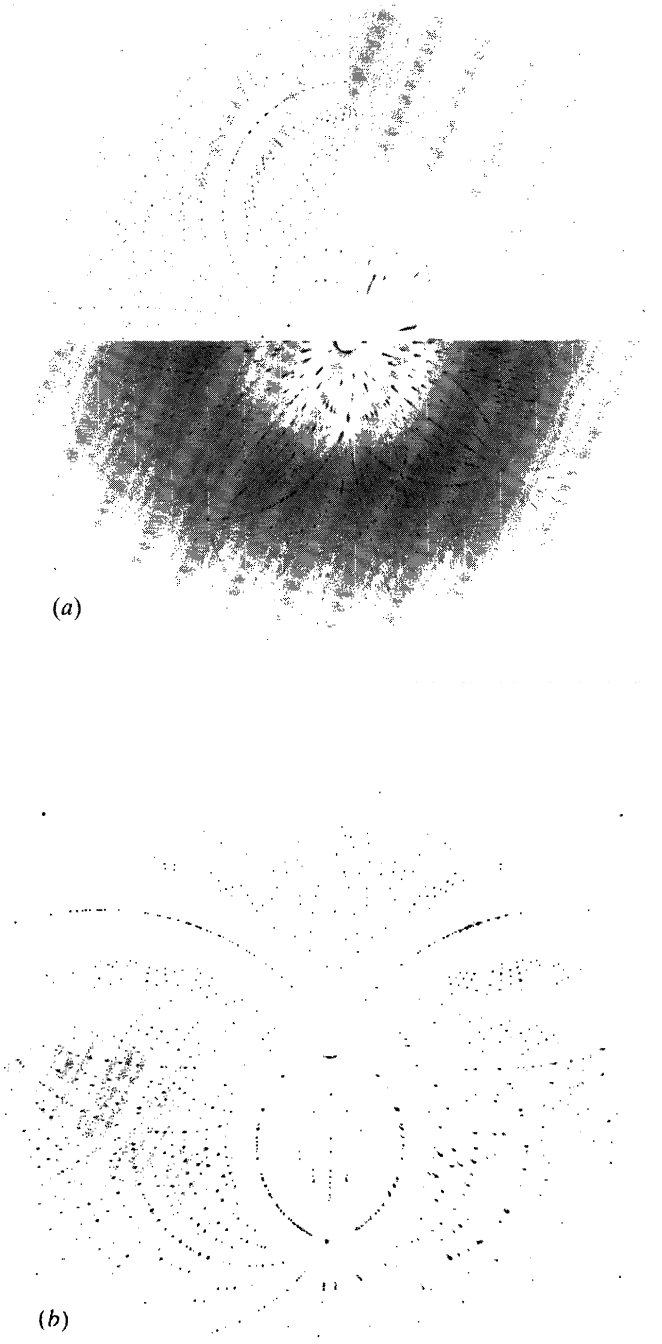

Figure 5. Composite images of exposures taken at beamlines X26-C and at X25. Details can be found in the text. (*a*) is from crystals of glutathione synthase. (*b*) is from crystals of hen egg-white lysozyme.

PHILOSOPHICAL TRANSACTIONS OF THE ROYAL SOCIETY A MATHEMATICAL, PHYSICAL & ENGINEERING SCIENCES

experienced damage *during* single 125 ms exposures. One such photograph is shown as the bottom half of the composite diffraction photograph, figure 5*a*. One can see evidence of damage in the streaking of reflections. None the less, two successive frames of usable data were obtained from a similar crystal on X26-C. In the top half of figure 5*a* are shown the first and third of 4 s exposures taken of this crystal on X26-C (the second film was very similar in appearance to the first).

Similar effects were observed several times with crystals of lysozyme at approximately 27 °C, mounted both wet and dry. This sort of experiment is extremely difficult to control and quantitate, but the difference was a factor between 1.5 and 2 in the number of frames that could be recorded. Composite photographs of lysozyme crystals are shown in figure 5*b*. The exposures on beamline X26-C (top half) were four seconds; the exposures for the bottom half, from X25, were 100 ms. The top-right was the seventh exposure taken from that crystal. Because we judge that the overall exposure of the films from X25 was roughly twice that of those from X26-C, we display the fourth exposure on the bottom right from X25. The qualitative impression is that more data could have been measured from X26-C. The same effect was evident but less dramatic for crystals photographed at 4 °C because even in the X25 beam, crystals were fairly robust at this temperature.

The clearest result, which is no surprise to crystallographers, is the dramatic effect of cooling the specimen. Over twice as many reflections could have been measured from crystals of lysozyme at lowered temperature. The effect is especially dramatic when the higher intensity beam is used.

A conclusion one must draw is that care must be taken in the choice of experimental conditions for Laue photography. If these results are borne out, the use of a very high flux source for very rapid data collection can only be justified by the demands of the kinetics, because the cost in crystal damage will be high. On the other hand, one could choose conditions at low temperature, which would likely slow the reaction to be studied and relax the kinetic demands. This not only would decrease the need for high-intensity X-rays but also would ameliorate their effects.

We acknowledge the gift of the glutathione synthase protein and advice about crystallization from Hiroaki Kato, Takaaki Nishioka and Yukiteru Katsube. P.T.S. was supported by an Alexander Hollaender Fellowship during much of this work. Beamlines X12-C and X26-C are supported by the Office of Health and Environmental Research of the U.S Department of Energy and by the National Science Foundation. Beamlines X25 and X26-C are supported by the Division of Basic Energy Sciences of the U.S. D.O.E., Contract DE-AC02-76CH-00016.

References

Berman, L. E., Hastings, J. B., Oversluizen, T. & Woodle, M. 1992 Optical design and performance of the X25 hybrid wiggler beam line at the NSLS. *Rev. Sci. Instr.* (In the press).

Brünger, A 1990 *X-PLOR reference manual*. Waltham, Massachusetts: Polygen.

Campbell, J. W., Clifton, I. J., Greenhough, T. J., Hajdu, J., Harrison, S. C., Liddington, R. C. & Shrive, A. K. 1990 Calcium-binding sites in tomato bushy stand virus visualized by Laue crystallography. *J. molec. Biol.* **214**, 627–632.

Clifton, I. J., Elder, M. & Hajdu, J. 1991 Experimental strategies in Laue crystallography. *J. appl. Crystallogr.* **24**, 267–277.

Farber, G. K., Machin, P., Almo, S. C., Petsko, G. A. & Hajdu, J. 1988 X-ray Laue diffraction from crystals of xylose isomerase. *Proc. natn. Acad. Sci. U.S.A.* **85**, 112–115.

Hajdu, J., Machin, P. A., Campbell, J. W., Greenhough, T. J., Clifton, I. J., Zurek, S., Gover, S., Johnson, L. N. & Elder, M. 1987 Millisecond X-ray diffraction and the first electron-density map from Laue photographs of a protein crystal. *Nature, Lond.* **329**, 178–181.

Hajdu, J. & Johnson, L. N. 1990 Progress with Laue diffraction studies on protein and virus crystals. *Biochem.* **29**, 1669–1678.

Helliwell, J. R., Habash, J., Cruickshank, D. W. J., Harding, M. M., Greenhough, T. J., Campbell, J. W., Clifton, I. J., Elder, M., Machin, P. A., Papiz, M. Z. & Zurek, S. 1989 The recording and analysis of synchrotron X-radiation Laue diffraction photographs. *J. appl. Crystallogr.* **22**, 483–497.

Howell, P. L., Almo, S. C., Petsko, G. A., Parsons, M. R. & Hajdu, J. 1990 Structure determination of turkey egg-white lysozyme using Laue diffraction. In *Proc. Amer. Crystallogr. Ass Fortieth Anniversary Meeting, Abstracts, ser.* 2 **18**, 38.

Kabsch, W. 1988 *J. appl. Crystallogr.* **21**, 916–924.

Kato, H., Yamaguchi, H., Hata, Y., Nishioka, T., Katsube, Y. & Oda, J. 1989 Crystallization and preliminary X-ray studies of glutathione synthetase from *Escherichia coli* B. *J. molec. Biol.* **209**, 503–504.

Mangel, W. F., Singer, P. T., Cyr, D. M., Umland, T. C., Toledo, D. L., Stroud, R. M., Pflugrath, J. W. & Sweet, R. M. 1990 Structure of an acyl-enzyme intermediate during catalysis: guanidinobenzoyl trypsin. *Biochem.* **29**, 8351–8357.

Messerschmidt, A. & Pflugrath, J. W. 1987 Crystal orientation and X-ray pattern prediction routines for area-detector diffractometer systems in macromolecular crystallography. *J. appl. Crystallogr.* **20**, 306–315.

Moffat, J. K. 1989 *A. Rev. Biophys. biophys. Chem.* **18**, 309–332.

Reynolds, C. D., Stowell, B. & Joshi, K. K. 1988 Preliminary study of a phase transformation in insulin crystals using synchrotron radiation Laue diffraction. *Acta crystallogr.* B **44**, 512–515.

Schlichting, I., Almo, S. C., Rapp, G., Wilson, K., Petratos, K., Lentfer, A., Wittinghofer, A., Kabsch, W., Pai, E. F., Petsko, G. A. & Goody, R. S. 1990 Time-resolved X-ray crystallographic study of the conformational change in Ha-Ras p21 protein on GTP hydrolysis. *Nature, Lond.* **345**, 309–315.

Stoddard, B. L., Koenigs, P., Porter, N., Petratos, K., Petsko, G. A. & Ringe, D. 1991 Observation of the light-triggered binding of a pyrone to chymotrypsin by Laue X-ray crystallography. *Proc. natn. Acad. Sci.* **88**, 5503–5507.

Sweet, R. M., Pflugrath, J. W., Wonacott, A. J. & Arndt, U. W. 1990 Use of a FAST are a diffractometer at a synchrotron X-ray source. In *Collected Abstracts 15th Cong. of Int. Union of Crystallogr.* C-10.

Szebenyi, D. M. E., Biderback, D., Le Grand, A., Moffat, K., Schildkamp, W. & Teng, T.-Y. 1988 120-Picosecond Laue diffraction using an undulator X-ray source. *Trans. Am. Crystallogr. Assoc.* **24**, 167–172.

Tronrud, D. E., Ten Eyck, L. F. & Matthews, B. W. 1987 *Acta crystallogr.* A **43**, 489.

Weissman, L. 1982 In *Computational crystallography* (ed. D. Sayre), pp. 56–63. Oxford University Press.

PHILOSOPHICAL TRANSACTIONS OF THE ROYAL SOCIETY A MATHEMATICAL, PHYSICAL & ENGINEERING SCIENCES

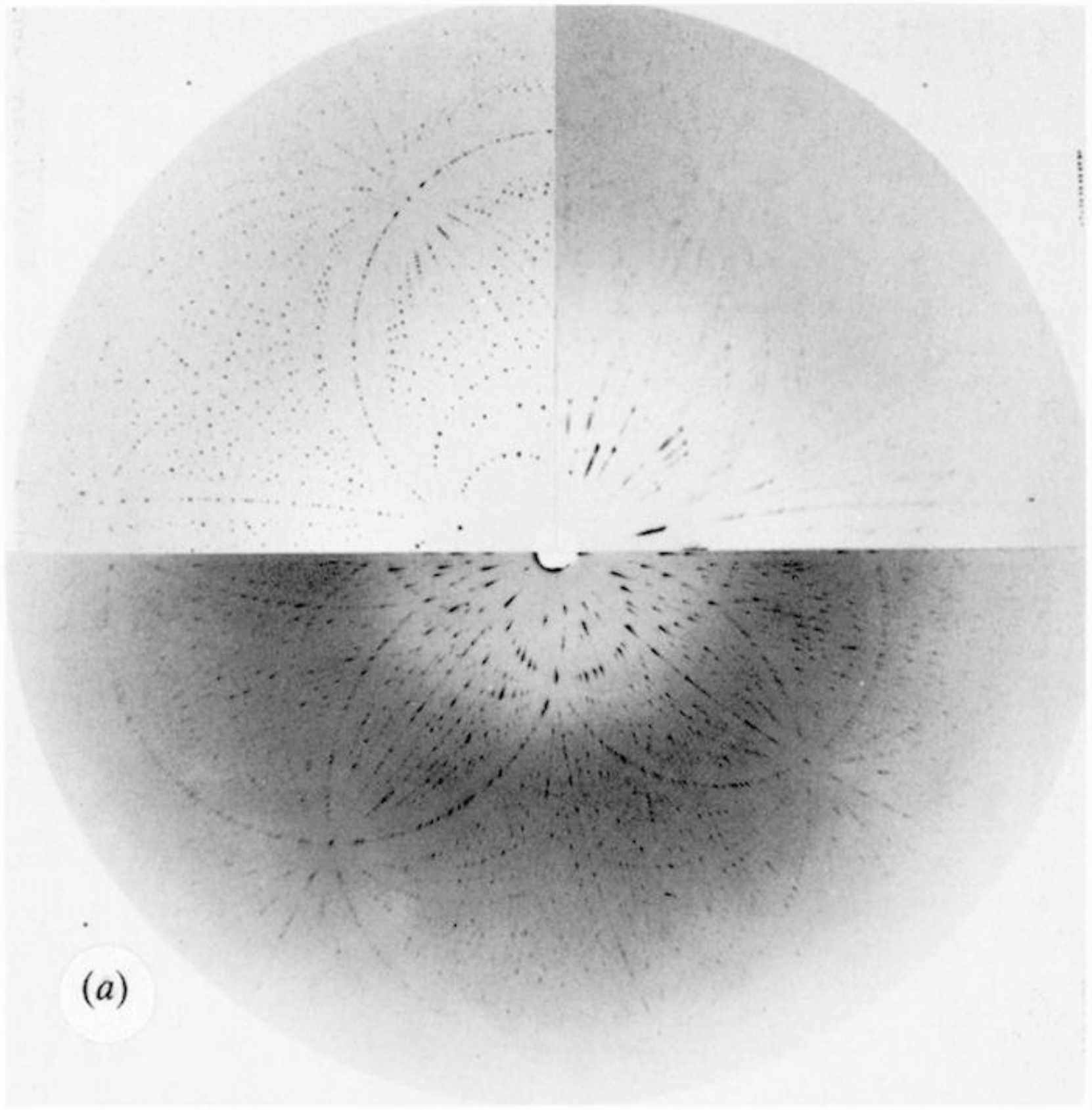

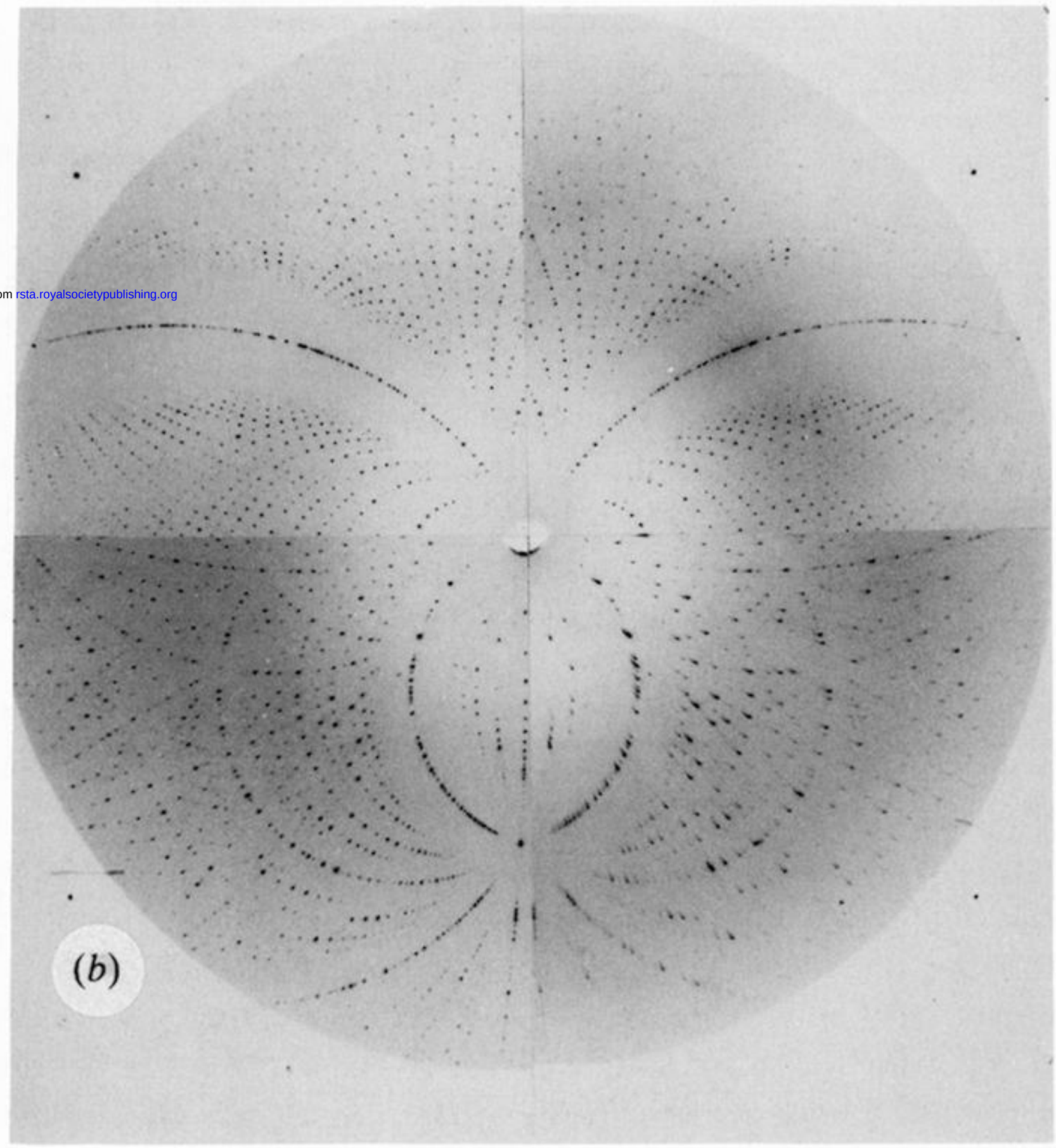

Figure 5. Composite images of exposures taken at beamlines X26-C and at X25. Details can be found in the text. (*a*) is from crystals of glutathione synthase. (*b*) is from crystals of hen egg-white lysozyme.